Inhibition of STAT-mediated cytokine responses to chemically-induced colitis prevents inflammation-associated neurobehavioral impairments

Ryusuke Sin [a], Naoki Sotogaku [a,1], Yoshinori N. Ohnishi [a], Takahide Shuto [a], Mahomi Kuroiwa [a], Yukie Kawahara [a], Keita Sugiyama [a], Yuki Murakami [b], Masaaki Kanai [c], Hiroshi Funakoshi [c], Ayanabha Chakraborti [d], James A Bibb [d], Akinori Nishi [a,*]

[a] Department of Pharmacology, Kurume University School of Medicine, Kurume, Fukuoka 830-0011, Japan
[b] Department of Hygiene and Public Health, Kansai Medical University, Hirakata, Osaka 573-1010, Japan
[c] Department of Advanced Medical Science, Asahikawa Medical University, Asahikawa, Hokkaido 078-8510, Japan
[d] Department of Translational Neuroscience, University of Arizona College of Medicine in Phoenix, Phoenix, AZ 85004-2230, USA

ARTICLE INFO

ABSTRACT

Depression can be associated with chronic systemic inflammation, and production of peripheral proinflammatory cytokines and upregulation of the kynurenine pathway have been implicated in pathogenesis of depression. However, the mechanistic bases for these comorbidities are not yet well understood. As tryptophan 2,3-dioxygenase (TDO) and indoleamine 2,3-dioxygenase (IDO), which convert tryptophan to kynurenine, are rate-limiting enzymes of the kynurenine pathway, we screened TDO or IDO inhibitors for effects on the production of proinflammatory cytokines in a mouse macrophage cell line. The TDO inhibitor 680C91 attenuated LPS-induced pro-inflammatory cytokines including IL-1β and IL-6. Surprisingly, this effect was TDO-independent, as it occurred even in peritoneal macrophages from TDO knockout mice. Instead, the anti-inflammatory effects of 680C91 were mediated through the suppression of signal transducer and activator of transcription (STAT) signaling. Furthermore, 680C91 suppressed production of proinflammatory cytokines and STAT signaling in an animal model of inflammatory bowel disease. Specifically, 680C91 effectively attenuated acute phase colon cytokine responses in male mice subjected to dextran sulfate sodium (DSS)-induced colitis. Interestingly, this treatment also prevented the development of anxiodepressive-like neurobehaviors in DSS-treated mice during the recovery phase. The ability of 680C91 to prevent anxiodepressive-like behavior in response to chemically-induced colitis appeared to be due to rescue of attenuated dopamine responses in the nucleus accumbens. Thus, inhibition of STAT-mediated, but TDO-independent proinflammatory cytokines in macrophages can prevent inflammation-associated anxiety and depression. Identification of molecular mechanisms involved may facilitate the development of new treatments for gastrointestinal-neuropsychiatric comorbidity.

1. Introduction

Inflammation accompanying peripheral immune activation is associated with psychiatric disorders including depression and anxiety (Beurel et al., 2020). Increases in peripheral proinflammatory cytokines such as IL-1, IL-6 and TNFα have been implicated in pathogenesis of depression (Howren et al., 2009; Köhler et al., 2017; Beurel et al., 2020). Patients with inflammatory bowel disease (IBD) including ulcerative colitis and Crohn's disease present with high prevalence of depression and anxiety (Neuendorf et al., 2016; Abautret-Daly et al., 2018; Barberio

et al., 2021). As evidence of this strongly-linked comorbidity continues to emerge, it is important to better understanding how inflammatory disorders can be treated so that depression susceptibility may be limited.

To study IBD pathogenesis and pharmacological therapies, animal models of IBD such as DSS-induced colitis have been used (Perše and Cerar, 2012). DSS, administered in drinking water, penetrates colon epithelial cells and induces the production of macrophage-derived cytokines such as IL-1β, IL-6, and TNFα without requiring T cell activation in the acute phase (Dieleman et al., 1994). The cytokine profiles correlate with clinical and histological parameters of DSS-induced colitis

(Perše and Cerar, 2012). Pathways that trigger the production of proinflammatory cytokines in macrophages are, thus, rational therapeutic targets for the control the intestinal inflammation in DSS-induced colitis.

Tryptophan is metabolized by two divergent pathways where it can either be converted to serotonin (5-hydroxytrypamine, 5-HT) or kynurenine. Unabsorbed tryptophan is metabolized by intestinal microorganisms into several molecules such as indole derivatives, tryptamine and skatole, which are aryl hydrocarbon receptor ligands (Modoux et al., 2021). The activation state of the kynurenine pathway is intertwined with inflammatory responses (Baumgartner et al., 2019). Furthermore, upregulation of the kynurenine pathway can occur in psychiatric disorders including depression and schizophrenia (Chen and Guillemin, 2009; Schwarcz et al., 2012; Cervenka et al., 2017). Kynurenine is produced from tryptophan by tryptophan 2,3-dioxygenase (TDO) or indoleamine 2,3-dioxygenase (IDO1/IDO2), and is the precursor to a series of tryptophan metabolites. Inflammation stimulates IDO induction in macrophages and dendritic cells, leading to an increase in kynurenine metabolites and corresponding decreases in tryptophan and 5-HT (Maes et al., 2011; Schwarcz et al., 2012).

Glucocorticoid production in response to stress increases TDO activity in the liver, causing tryptophan and 5-HT depletion in the plasma and brain (Maes et al., 2011; Ohta et al., 2017). Tryptophan and 5-HT levels are elevated in the plasma and brain (midbrain and hippocampus) of TDO knockout mice, which exhibit reduced anxiety-related behaviors (Kanai et al., 2009; Hattori et al., 2018). When the kynurenine pathway is upregulated, the increased kynurenine in plasma crosses the blood–brain barrier, triggering the synthesis of excitotoxic metabolites such as quinolinic acid by microglia with corresponding reduction in brain 5-HT synthesis (Maes et al., 2011; Schwarcz et al., 2012). Quinolinic acid causes neuronal excitotoxicity and induces the production of reactive oxygen species (ROS) and nitric oxide (NO), leading to the oxidation of tetrahydrobiopterin (BH4) and the reduction of brain dopamine synthesis (Felger and Treadway, 2017). Thus, the upregulation of the kynurenine pathway results in the increased susceptibility to depression.

Kynurenine can act as an oncometabolite in the colon, facilitating an immunologically susceptible microenvironment for neoplastic cells to survive and invade surrounding tissue (Ala, 2021). Thus, TDO and/or IDO inhibitors are being actively developed as potential cancer immunotherapies (Cheong and Sun, 2018; Kim and Tomek, 2021). However, given the interaction between inflammation, kynurenine metabolism, and neuropsychiatric disorders, we hypothesized that drugs targeting the kynurenine pathway might also serve as potential treatments for mood disorders, and depression associated with inflammation in particular. To test this, we conducted *ex vivo* and *in vivo* studies that link inflammation to anxiodepressive-like behaviors and suggest that anti-inflammation therapy may disrupt gastrointestinal inflammation-depression comorbidity.

2. Materials and methods

2.1. Animals

Male C57BL/6J mice were purchased from CLEA Japan (Tokyo, Japan). Male wild-type and TDO knockout mice were obtained from breeding pairs of heterozygous knockout mice (Kanai et al., 2009). Mice at 8–12 weeks of age were used. Mice were housed 2–4 per cage and were maintained on a 12-h light/dark cycle (lights on from 7:00 am to 7:00 pm) with access to food and water *ad libitum*. All mice used in this study were handled in accordance with the Guide for the Care and Use of Laboratory Animals as adopted by the U.S. National Institutes of Health, and the specific protocols were approved by the Institutional Animal Care and Use Committee of Kurume University School of Medicine.

2.2. Preparation of mouse peritoneal macrophages

Peritoneal macrophages were prepared from thioglycollate-elicited peritoneal cells in wild-type and TDO knockout mice, as previously reported (Koga et al., 2013). Mice were intraperitoneally injected with 2 mL of 4% thioglycollate (Sigma-Aldrich, St. Louis, MO). Peritoneal exudate cells were collected from the peritoneal cavity 3 or 4 days after injection and the cell suspension in complete medium (RPMI1640 medium supplemented with 10% fetal bovine serum) were incubated in 35 mm culture dish. After 2 h, the cells were washed three times with PBS and cultured in the complete medium. The adherent cells were used as peritoneal macrophages for the experiments.

After 24 h of culture, peritoneal macrophages were incubated with vehicle or a TDO inhibitor, 680C91 (1, 10, 50 µM) (Tocris Bioscience, Bristol, UK). After 30 min of incubation, lipopolysaccharide (LPS) (FUJIFILM Wako, Osaka, Japan) at 100 ng/ml was added and the macrophages were incubated for 5 h. The peritoneal macrophages were harvested for mRNA assays.

2.3. Cell culture of Raw 264.7 cells and THP-1 cells

Raw 264.7 cells, which are macrophage-like cell line derived from Balb/c mice, were seeded in RPMI1640 medium supplemented with 10% fetal bovine serum in 35 mm culture dish. Raw 264.7 cells were maintained at 37 °C in humidified 95% air/5% CO$_2$. After 24 h of culture, Raw 264.7 cells were incubated with vehicle, a TDO inhibitor [6-Fluoro-3-((1E)-2-(3-pyridinyl)ethenyl)-1H-indole (680C91; 1, 10, 50 µM) or *trans*-6-Fluoro-3-(2-(1H-tetrazol-5-yl)vinyl)-1H-indole (LM10; 10, 50 µM) (Selleck, Houston, TX)], an inhibitor of IDO/TDO pathway and IDO2 [1-methyl-D-tryptophan (D-1-MT; 1, 10 µM) (Sigma-Aldrich)] (Fox et al., 2018), or an IDO1 inhibitor [epacadostat (1, 10 µM) (AdipoGen Life Sciences, San Diego, CA)] for 30 min. After 30 min of incubation, LPS at 100 ng/ml was added and the cells were incubated for 5 h. The cells were harvested for mRNA and/or protein assays.

THP-1 cells, a human monocytic leukemia-derived cell line, were cultured in RPMI1640 supplemented with 10% fetal bovine serum in 35 mm culture dishes. To induce monocytes differentiated into macrophages, cells were incubated with phorbol 12-myristate 13-acetate (PMA) (Sigma-Aldrich) at a concentration of 10 ng/ml for 48 h. The THP-1-derived macrophages were then treated with vehicle, 680C91 (10 µM) or epacadostat (10 µM) for 30 min. After 30 min of incubation, LPS at 100 ng/ml was added and the cells were incubated for 5 or 24 h and harvested for measurements of tryptophan and kynurenine.

2.4. Dextran sulfate sodium (DSS)-induced colitis in mice

Acute colitis was induced by DSS in C57BL/6J mice or wild-type and TDO knockout mice. 3% DSS (MW 36–50 kD, MP Biomedicals, Irvine, CA) was administered in drinking water for 8 days, as previously described (Theiss et al., 2011; Chassaing et al., 2014). Vehicle control (saline containing 1% DMSO, 5% PEG 400, 5% Tween 20) or 680C91 (8 mg/kg, 0.05 mL/10 g body weight) was administrated intraperitoneally (i.p.) once a day for 8 consecutive days (day 1–8). The dose of 680C91 *in vivo* was chosen based on previous reports (Salter et al., 1995; Bessede et al., 2014; Abuin-Martínez et al., 2021). On day 8, the mice were sacrificed, and the colon from ileocecum to 1 cm above the anus was dissected. The colon length was measured, and tissues from the mid colon were collected for mRNA and protein assays. As traces of DSS in RNA preparations from colon tissues have been known to interfere with PCR amplification, DSS traces were removed by double precipitation of RNA with LiCl using the modified RNA cleaning protocol (Oldak et al., 2018).

2.5. Quantitative real-time PCR

Total RNA was isolated from peritoneal macrophages, Raw 264.7

cells and colon tissues using Sepasol RNA I Super G (Nacalai Tesque, Kyoto, Japan). After genomic DNA cleaning, cDNA was obtained by total RNA reverse transcription using a QuantiTect Reverse Transcription Kit (Qiagen, Valencia, CA). Real-time PCR was performed using LightCycler 480 System II (Roche, Basel, Switzerland) with GeneAce SYBR qPCR Mix α No ROX (NIPPON GENE CO., LTD., Tokyo, Japan) for IL-1β, IL-6 and TNFα or QuantiFast SYBR Green PCR Master Mix (Qiagen, Valencia, CA) for TDO. The primer sequences are listed in Table A.1. The relative mRNA levels of individual samples were calculated with the comparative Ct method ($2^{-\Delta\Delta Ct}$).

2.6. Western blot analysis

Raw 264.7 cells were lysed with RIPA buffer. Colon tissues were sonicated in boiling 1% sodium dodecyl sulfate (SDS) containing 50 mM sodium fluoride and boiled for an additional 10 min. Small aliquots of the homogenate were retained for protein determination using the BCA protein assay method (Pierce, Rockford, IL). The protein was separated by SDS-PAGE, and transferred to nitrocellulose membranes. The membranes were immunoblotted using phosphorylation state-specific antibodies for phospho-Tyr701 STAT1 (sc-136229, 1:1,000, Santa Cruz Biotechnology, Dallas, TX) and phsopho-Tyr705 STAT3 (#9145, 1:2,000, Cell Signaling) and antibodies generated against Pro-IL1β (AF-401-NA, 1:1,000, R&D Systems, Minneapolis, MN), STAT1 (sc-464, 1,1000, Santa Cruz Biotechnology), STAT3 (#9139, 1:1,000, Cell Signaling Technology, Danvers, MA) and β-actin (#4970, 1:2,000 dilution, Cell Signaling Technology; 66009–1-Ig, 1:1,000 dilution, Proteintech, Rosemont, IL). The membrane was incubated with a goat anti-mouse or rabbit Alexa 680-linked IgG (1:5,000 dilution, Thermo Fisher Scientific, Waltham, MA), a donkey anti-Goat Alexa 680-linked IgG (1:5,000 dilution, Thermo Fisher Scientific) or a goat anti-mouse or rabbit IRDye800-linked IgG (1:5,000 dilution, Thermo Fisher Scientific). Fluorescence at infrared wavelengths was detected by the Odyssey infrared imaging system (LI-COR, Lincoln, NE) and quantified using the Odyssey software.

2.7. Behavioral analyses

2.7.1. Elevated plus maze test (EPM)
The apparatus of elevated plus maze consists of two open arms (25 × 8 cm) and two closed arms (25 × 8 × 15 cm) elevated 65 cm above the floor. Each mouse was placed in the center facing the open arms and allowed to explore for 5 min. The time spent in the open arms and the number of open arm entries were measured using SMART Video Tracking System (Panlab, Barcelona, Spain).

2.7.2. Open field test (OFT)
A white plexiglas box (42 × 42 × 42 cm) was used for the open field test. Each mouse was introduced into the center of the chamber at the beginning of the test and the time spent in central zone and total traveled distance in 10 min were measured using SMART Video Tracking System.

2.7.3. Tail suspension test (TST)
The mice were suspended by their tails from a metal rod, 60 cm above the surface of table with an adhesive tape. After 1 min acclimatization, the immobility time was recorded for 5 min.

2.7.4. Sucrose preference test (SPT)
The mice were singly housed during 4 days of task, and were presented with two bottles, containing tap water or a 1.0% sucrose solution. After habituation to consume liquid from small bottles for 2 days, the sucrose preference was measured during the next 2 days. To prevent a possible place preference, the positions of two bottles were switched each day. The sucrose preference over the 2 days of period was calculated as [average sucrose solution intake (g) / average total liquid intake (g)] × 100.

2.8. Dopamine measurement with in vivo microdialysis

Microdialysis probes [I-shaped cannulas: customized home-made probes using dialysis membrane (Hospal Industrie, Meyzieu, France)] were implanted in the unilateral nucleus accumbens (NAc) (exposed length 1.5 mm) of mice under xylazine (8 mg/kg, i.p.) and sevoflurane (2–5%) anesthesia and local application of 0.1% lidocaine. The coordinates of the implantation were A/P + 1.4 mm, L/M 0.6 mm from the bregma and V/D −4.5 mm from the dura to target the NAc (Paxinos and Franklin, 2004). After surgery, the mice were housed individually in plastic cages (30 × 30 × 40 cm) for recovery.

Microdialysis experiments were performed 3 or 4 days after implantation of the probe as previously described (Hanada et al., 2018). An online approach for real-time quantification of dopamine was used. The flow rate of Ringer's solution was 2.0 μl/min. The 20-min sample fractions collected through the dialysis probes were directly injected to high-performance liquid chromatography using a reverse-phase column (150 × 4.6 mm, Supelcosil LC18; Merck, Darmstadt, Germany) with electrochemical detection. An LC-20AD pump (Shimadzu Corporation, Kyoto, Japan) was used in conjunction with an electrochemical detector (potential of the first cell, +180 mV; potential of the second cell, −180 mV) (ESA, Chelmsford, MA). The mobile phase was a mixture of 4.1 g/L sodium acetate adjusted to pH 4.1, 100 mg/L Na$_2$EDTA, 120 mg/L octanesulfonic acid and 10% methanol. The flow rate was 0.4 mL/min. The detection limit of the assay was approximately 0.9 fmol per sample (on-column). The composition of Ringer's solution was (in mM) NaCl 140.0, KCl 4.0, CaCl$_2$ 1.2, and MgCl$_2$ 1.0. At the end of the experiments, the mice were given an overdose of sevoflurane, and the brains were fixed with 4% paraformaldehyde via intracardiac infusion. Coronal sections (50 μm) were cut, and dialysis probe placement was localized using the atlas of Paxinos and Franklin (Paxinos and Franklin, 2004). Misplacement of the microdialysis probes was not observed in any experimental animals used for the study.

2.9. Rewarding stimuli

Dopamine in the NAc were measured in response to cocaine infusion into the NAc (Hanada et al., 2018) and rewarding stimuli such as palatable food and exposure to a female mouse.

2.9.1. Palatable food
After microdialysis probe implantation, approximately 1 g of Home Pie (Fujiya, Tokyo, Japan), to which mice exhibit palatability, was introduced to the mice to promote habituation. During the experimental period, after obtaining three stable consecutive samples of dopamine, the mice were exposed to approximately 1 g of palatable food for 20 min. After 20 min, leftover palatable food was removed, while the mouse had free access to regular food and water all the time (Kawahara et al., 2013; Hanada et al., 2018).

2.9.2. Exposure to a female mouse
During the experimental period, male mice were exposed to female C57BL/6N mice at the same age, purchased from Japan SLC (Shizuoka, Japan), after obtaining three stable consecutive samples of dopamine. Female mice enclosed in a clear acrylic cage (10 × 10 × 20 cm) with 1 cm slits were placed in the plastic cage (30 × 30 × 40 cm) of male mouse for 20 min, and thereafter, the female mouse and the clear acrylic cage were removed (Hanada et al., 2018).

2.10. Measurements of tryptophan and kynurenine in THP-1-derived macrophages

Tryptophan and kynurenine were measured in THP-1-derived macrophages, as previously described (Murakami et al., 2021). THP-1-derived macrophages were sonicated with 500 μl of homogenization buffer (20 mM potassium phosphate buffer, pH 7.0, containing 0.14 M

KCl). The cell lysates were centrifuged (14,000 rpm × 20 min, 4 °C), and the supernatant was collected. Small aliquots of the supernatant were retained for protein determination using the BCA protein assay method (Pierce, Rockford, IL). The supernatant was diluted (1:2, v/v) in 10% perchloric acid (FUJIFILM Wako, Osaka, Japan) for measurements of tryptophan and kynurenine. After through mixing, the precipitated proteins were removed by centrifugation (14,000 rpm × 20 min, 4 °C), and 40 µl of liquid above the precipitation was subjected to high-performance liquid chromatography (HPLC) analysis for measurements of tryptophan and kynurenine. Tryptophan and kynurenine were gradient-eluted from a reverse-phase chromatography column (CAP-CELL PAK ADME S3, 100 mm [L] × 2.1 mm [internal diameter; ID], 3-µm particle size, Osaka Soda Co., LTD, Osaka, Japan) with a mobile phase containing 10 mM ammonium formate buffer (pH 4.0), and 0–25% (v/v) gradient of acetonitrile at a flow rate of 0.2 mL/min. Tryptophan and kynurenine were detected using an ultraviolet and visible spectrophotometric detector (UV detector, SPD-20A, Shimadzu Co., Kyoto, Japan) (UV wavelength for TRP: 280 nm, for KYN: 254 nm).

2.11. Statistical analysis

The data are displayed as Mean ± S.E.M. The significance of differences within each group was determined with one-way ANOVA followed by Bonferroni post hoc test. When two groups were compared, Student's *t*-test or two-way ANOVA followed by Bonferroni *post hoc* test was used. The analyses were performed using Prism 7.0 software (GraphPad Software, San Diego, CA). For analyses of microdialysis data, all values were expressed as a percentage of the basal values (100%), obtained as the average of three stable baseline samples. The values obtained after cocaine infusion or exposure to palatable food or female mouse were compared with the basal values using mixed linear models with the measurement time as a covariate, and Bonferroni's correction was applied for multiple comparisons using the SAS MIMED procedure (Version 9.4, SAS Institute, Cary, NC). Repeated measures two-way ANOVA were used to compare the experimental groups (JMP Pro, SAS Institute). $p < 0.05$ was considered to be significant. Details of the statistical analysis are listed in Table A.2.

3. Results

3.1. Suppression of the expression of pro-inflammatory cytokine mRNAs in LPS-treated Raw 264.7 cells by 680C91, but not other TDO or IDO inhibitors

To better understand the link between inflammation and kynurenine metabolism, we assessed the effects of TDO inhibitor treatment of macrophage-like Raw 264.7 cells on LPS-induced cytokine gene expression (Fig. 1A). As one TDO inhibitor that was readily commercially available, we chose 680C91. LPS stimulation of Raw 264.7 cells for 5 h induced the expression of IL-1β, IL-6 and TNFα mRNAs (Fig. 1B-D). Treatment of Raw 264.7 cells with 680C91 suppressed the LPS-induced expression of IL-1β and IL-6 mRNAs (Fig. 1B, C), but not of TNFα mRNA (Fig. 1D), without affecting the basal expression of IL-1β, IL-6 or TNFα mRNA (Fig. 1E-G). Toward validation that 680C91 was acting to attenuate cytokine responses in these cells, TDO mRNA was quantitated. Somewhat surprisingly, the expression of TDO mRNA in Raw 264.7 cells was below the limit of PCR detection (Fig. 1H), suggesting that 680C91 has the ability to suppress LPS-induced expression of proinflammatory cytokines via TDO-independent mechanisms. In contrast, another TDO inhibitor, LM10, or an inhibitor of IDO/TDO pathway and IDO2, D-1-MT, did not suppress the LPS-induced expression of IL-1β, IL-6 or TNFα mRNA in Raw 264.7 cells (Fig. 1B-D, 1I-K), although an IDO1 inhibitor, epacadostat, slightly suppressed the LPS-induced expression of IL-1β and IL-6 mRNAs at the high concentration (10 µM) (Fig. 1I-K). The TDO-independent suppression of LPS-induced expression of proinflammatory cytokines seems to be specific features

of 680C91 among the classes of TDO or IDO1 inhibitors, although not all TDO or IDO1 inhibitors tested.

To be sure that 680C91 and epacadstat have abilities to inhibit TDO and IDO1 in cells, respectively, THP-1cells, which are known to express TDO and IDO1 (Fujigaki et al., 2006; Hoffmann et al., 2019), were stimulated with LPS for 5 and 24 h, and the production of kynurenine from tryptophan was evaluated in the presence of 680C91 or epacadstat (Fig. A.1A). LPS stimulation for 5 h did not affect the production of kynurenine from tryptophan, but 680C91 and epacadstat reduced the kynurenine contents below the basal levels (Fig. A.1B-D). After 24 h of LPS stimulation, kynurenine contents were increased by ~5-fold, and the increases of kynurenine contents and kynurenine/tryptophan ratio were abolished by 680C91 or epacadstat (Fig. A.1E-G). These results suggest that 680C91 regulates cellular function via TDO-dependent and independent mechanisms.

3.2. 680C91 down-regulates the expression of pro-IL-1β protein and the LPS signaling pathway in LPS-treated Raw 264.7 cells

Next, we examined the effects of 680C91 on the LPS-induced expression of pro-IL-1β protein, a precursor of IL-1β, and the LPS-induced phosphorylation of STAT1 and STAT3, which were known to play a role in IL-1β induction (Lee et al., 2006; Samavati et al., 2009). Treatment of Raw 264.7 cells with LPS markedly increased the protein levels of pro-IL-1β (Fig. 2A) and the phosphorylation of STAT1 at Tyr701 (Fig. 2B) and STAT3 at Tyr705 (Fig. 2C). The LPS-induced increases in pro-IL-1β and p-STAT1 were suppressed by 680C91 (Fig. 2A, B). In addition, 680C91 showed the tendency to suppress the LPS-induced increases in p-STAT3 (Fig. 2C). We also examined the expression of IFN regulatory factor 3 (IRF3), p38 mitogen-activated protein (MAP) kinase, extracellular signal-regulated kinase (ERK), nuclear factor-κB (NF-κB), Akt, p70 S6 kinase (p70S6K) and interferon β (IFNβ), which are known as intracellular activation factors induced by LPS (Akira et al., 2006; Qin et al., 2016). 680C91 had no detectable effect on the LPS-induced expression of these inflammation-related genes (data not shown). These results confirm that 680C91 suppresses the expression of IL-1β and the activation of LPS signaling molecules.

3.3. 680C91 suppresses the expression of LPS-induced pro-inflammatory cytokine mRNAs in peritoneal macrophages prepared from wild-type and TDO KO mice

To investigate whether TDO is involved in anti-inflammatory action of 680C91 or not, peritoneal macrophages prepared from wild-type and TDO KO mice were stimulated with LPS in the absence or presence of 680C91 (Fig. 3A). LPS stimulation of peritoneal macrophages induced the expression of IL-1β, IL-6 and TNFα mRNAs in both wild-type and TDO KO mice (Fig. 3B-D). Treatment of peritoneal macrophages with 680C91 dose-dependently suppressed the LPS-induced expression of IL-1β and IL-6 mRNAs similarly in wild-type and TDO KO mice (Fig. 3B, C). The expression of TNFα mRNA was increased by 680C91 at the highest concentration (50 µM) in both wild-type and TDO KO mice (Fig. 3D). Interestingly, the TDO inhibitor, 680C91, suppressed the LPS-induced expression of IL-1β and IL-6 mRNAs in peritoneal macrophages from TDO KO mice as well as from wild-type mice. Therefore, we measured the expression of TDO mRNA in peritoneal macrophages and found that the expression levels of TDO mRNA was extremely low or below the limit of PCR detection in peritoneal macrophages from wild-type mice (Fig. 3E).

3.4. 680C91 attenuates the inflammatory responses in the acute phase of DSS-induced colitis

The *ex vivo* studies investigating the anti-inflammatory effects of TDO inhibitors yielded a surprising result, in that one compound, 680C91 attenuated inflammatory responses by macrophage-like cells
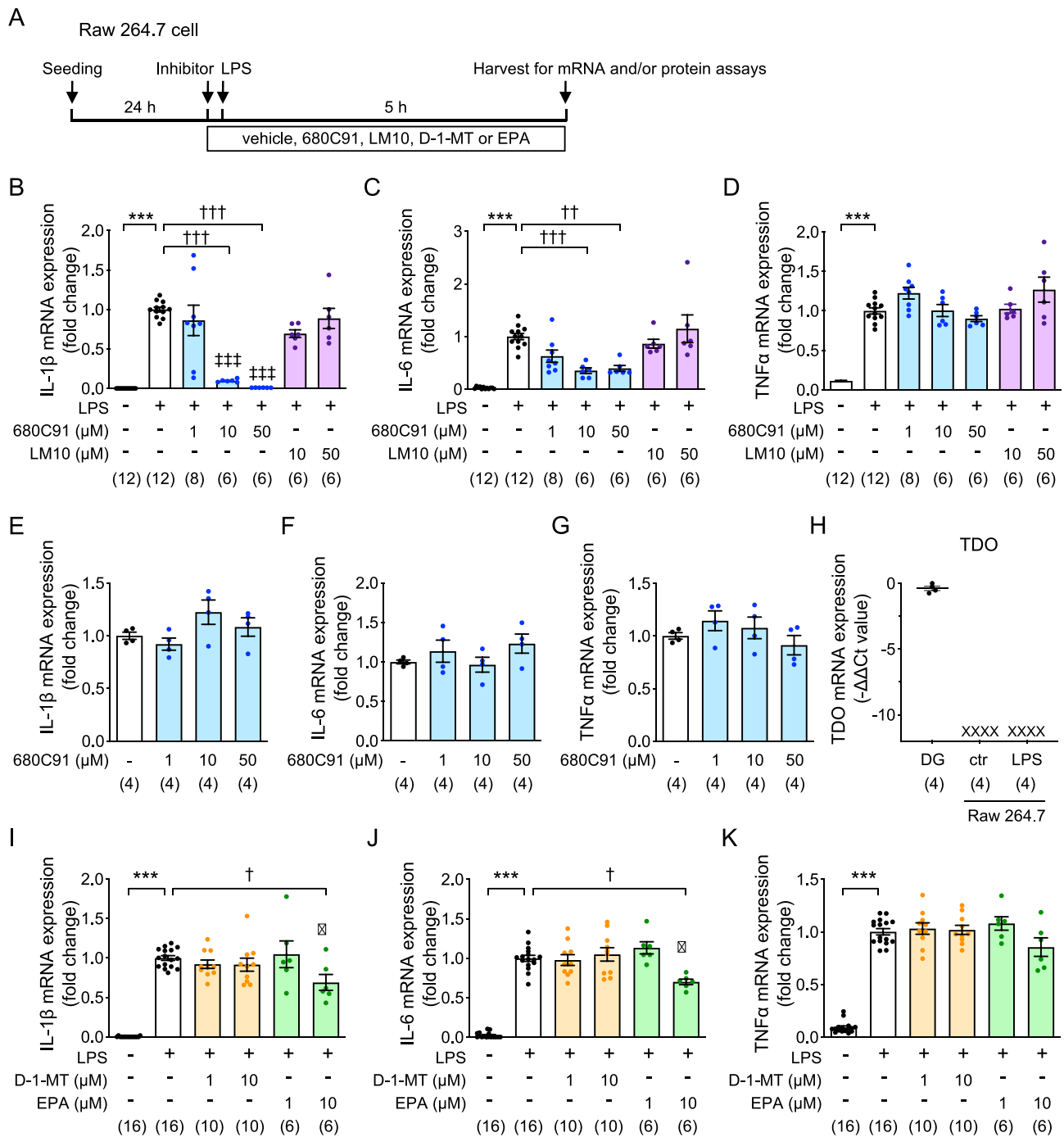
Fig. 1. Effects of TDO inhibitors, 680C91 and LM10, and IDO inhibitors, 1-MT and epacadostat, on the expression of pro-inflammatory cytokine mRNAs in LPS-treated Raw 264.7 cells. (A) Experimental design for treatment of Raw 264.7 cells with LPS and TDO/IDO inhibitors. (B-D) Effects of the TDO inhibitor, 680C91 (1, 10, 50 μM) or LM10 (10, 50 μM), on the mRNA levels of IL-1β (B), IL-6 (C) and TNFα (D) in LPS-treated Raw 264.7 cells. After 30 min of incubation with 680C91 or LM10, Raw 264.7 cells were stimulated with LPS at 100 ng/ml for 5 h in the continuous presence of 680C91 or LM10. The mRNA levels were normalized to LPS alone treatment. (E-G) Effects of 680C91 alone (1, 10, 50 μM) on the mRNA levels of IL-1β (E), IL-6 (F) and TNFα (G) in LPS-untreated Raw 264.7 cells. The mRNA levels were normalized to those without 680C91. (H) TDO mRNA expression in the hippocampal dentate gyrus (DG) from C57Bl/6J mice and Raw 264.7 cells. The TDO mRNA levels are normalized to those in the DG and are expressed as $-\Delta\Delta Ct$ values. ×, not detected. (I-K) Effects of the IDO inhibitor, 1-MT (1, 10 μM) or epacadostat (EPA; 1, 10 μM), on the mRNA levels of IL-1β (I), IL-6 (J) and TNFα (K) in LPS-treated Raw 264.7 cells. After 30 min of incubation with 1-MT or epacadostat, Raw 264.7 cells were stimulated with LPS at 100 ng/ml for 5 h in the continuous presence of 1-MT or epacadostat. The mRNA levels were normalized to LPS alone. Data represent mean ± SEM, and the number of experiments in each group is provided under columns. ***$p < 0.001$ vs. the control group; Student's t-test. †$p < 0.05$, ††$p < 0.01$, †††$p < 0.001$ vs. the group with LPS alone; ‡‡‡$p < 0.001$ vs. the group with LPS/680C91 (1 μM); §$p < 0.05$ vs. the group with LPS/epacadostat (1 μM); owe-way ANOVA and Bonferroni multiple comparison test.
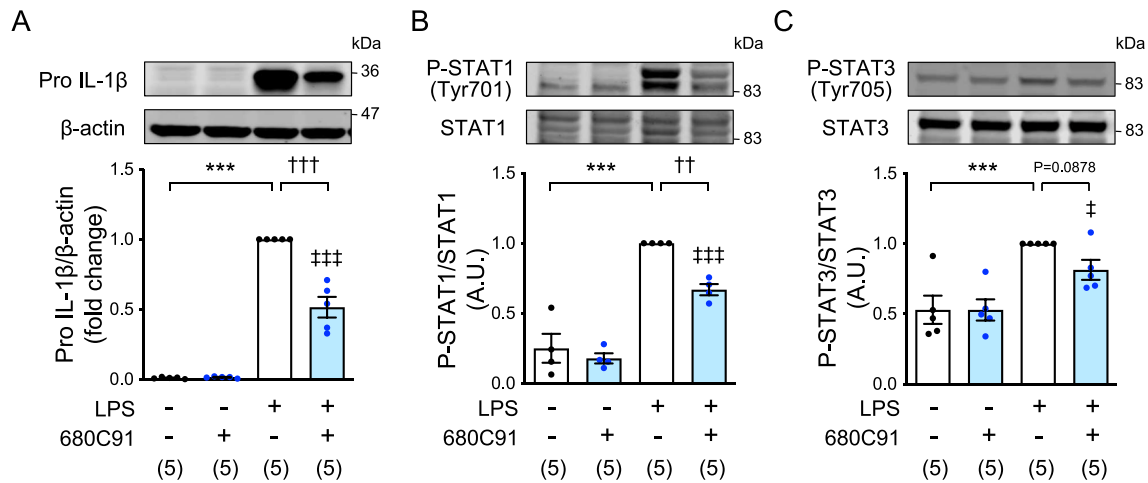
Fig. 2. Effects of 680C91 on the expression of pro-IL-1β and the phosphorylation of STAT1 and STAT3 in LPS-treated Raw 264.7 cells. The effects of 680C91 on the LPS-induced increases in the protein levels of pro-IL-1β and the phosphorylation of STAT1 and STAT3 were examined in Raw 264.7 cells. After 30 min of incubation with 680C91 (10 μM), cells were stimulated with LPS at 100 ng/ml for 5 h in the continuous presence of 680C91.Typical blots for pro-IL-1β (A), p-STAT1 at Tyr701/total STAT1 (B) and p-STAT3 at Tyr705/total STAT3 (C) are shown with quantitation. The protein levels of pro-IL-1β were normalized to β-actin and the group with LPS alone, and p-STAT1 and p-STAT3 were normalized to the corresponding total proteins and the group with LPS alone. Data represent mean ± SEM, and the number of experiments in each group is provided under columns. $^{***}p < 0.001$ vs. the control group; $^{†††}p < 0.001$ vs. the group with LPS alone; $^{‡}p < 0.05$, $^{‡‡‡}p < 0.001$ vs. the group with 680C91 alone; two-way ANOVA and Bonferroni multiple comparison test.

through undefined TDO independent actions. Given the link between bowel inflammation and mood disorders in humans, we wondered if the anti-inflammatory effects of 680C91 might be used to uncouple gut-brain comorbidity. To test this hypothesis, the anti-inflammatory effects of 680C91 *in vivo* were first examined in the acute phase of DSS-induced colitis (Fig. 4A). Systemic administration of 680C91 (i.p.) from Day 1 to 8 prevented the loss of body weight (Fig. 4B) and the shortening of colon length (Fig. 4C) in mice treated with DSS for 8 days (Day 1–8). DSS markedly increased the mRNA expression of IL-1β (Fig. 4D), IL-6 (Fig. 4E) and TNFα (Fig. 4F) in colon tissues obtained on Day 9. Similar to the effects observed in cultured cells, administration of 680C91 suppressed the DSS-induced increases in pro-inflammatory cytokine mRNAs (Fig. 4D-F). DSS also increased the protein levels of pro-IL-1β (Fig. 4G, H) and the phosphorylation of STAT1 at Tyr701 and STAT3 at Tyr705 without affecting the protein levels of STAT1 and STAT3 (Fig. 4I-K). Administration of 68,091 suppressed the DSS-induced increases in pro-IL-1β and the phosphorylation of STAT1 and STAT3 (Fig. 4G-4 K). These findings demonstrate that 680C91 attenuates the inflammation of colon and inflammatory responses of cytokines and the STA1/STAT3 signaling pathway in mice in the acute phase of DSS-induced colitis.

The effects of 680C91 were examined in the acute phase of DSS-induced colitis in wild-type and TDO KO mice (Fig. A.3A). 680C91 administration attenuated the DSS-induced shortening of colon length (Fig. A.3B) and the DSS-induced increases in the expression of IL-1β and IL-6 mRNAs (Fig. A.3C-E) in TDO KO mice as well as wild-type mice. The results suggest that 680C91 inhibits inflammatory responses in DSS-induced colitis via TDO-independent mechanisms *in vivo*.

3.5. Inflammatory responses of DSS-induced colitis in the recovery phase

After 21 days of recovery time from last DSS administration, the weight loss and the shortening of colon length in the DSS group observed on Day 9 were returned to the similar levels with those in the control group on Day 30 (Fig. 5B, C). In colon tissues, the levels of IL-1β and IL-6 mRNAs were still increased in the DSS group on Day 30, but the increase was much smaller than those in the acute phase (0.4% of IL-1β mRNA and 3.6% of IL-6 mRNA compared with those in the DSS group on Day 9) (Fig. 5D, E). 680C91 suppressed the small DSS-induced increases in IL-1β and IL-6 mRNAs. The effects of DSS on TNFα mRNA were not detected

on Day 30 (Fig. 5F). Except the slight increases in p-STAT3 in the DSS group, DSS and/or 680C91 induced no obvious effects on the protein levels of pro-IL-1β (Fig. 5F) or the phosphorylation of STAT1 (Fig. 5G) or STAT3 (Fig. 5H) on Day 30. These findings suggest that the inflammatory responses to DSS largely subside in the recovery phase of DSS-induced colitis, and the prolonged slight induction of pro-inflammatory cytokines were suppressed by 680C91.

3.6. Effects of 680C91 on anxiodepressive-like behaviors in the recovery phase of DSS-induced colitis

We next investigated the effects of 680C91 on anxiodepressive-like behaviors in the acute phase (Day 8 and 9) of DSS-induced colitis (Fig. 4A). DSS-treated mice showed behavioral impairments including decreased time spent in the open arms in the EPM (Fig. A.2A-C), decreased locomotor activity in the OFT (Fig. A.2D, E) and increased immobility time in the TST (Fig. A.2F) compared with control mice. 680C91 administration suppressed the attenuated struggle behavior in the TST, but did not affect the anxiogenic behaviors induced by DSS in the EPM. In addition, DSS-treated mice showed decreased overall locomotor activity, as a possible sickness behavior produced in the acute phase of DSS-induced colitis.

To avoid the influences of acute inflammation of DSS-induced colitis on behaviors, behavioral tests were conducted after 21 days of recovery time from last DSS administration (Day 29 and 30). Despite this delay, DSS treatment-induced decreases in the number of open arm entries and the time spent in the open arm in the EPM (Fig. 6A, B) and decreases in the time spent in central zone in the OFT (Fig. 6D) compared with control mice persisted as behavioral maladaptations. 680C91 suppressed the anxiety-like behaviors in DSS-treated mice. We also noted that mice treated with 680C91 alone showed mild anxiety-like behaviors in the EPM (Fig. 6A, B), possibly due to altered tryptophan metabolism. The locomotor activity in the OFT and EPM were moderately decreased in DSS-treated mice (Fig. 6C, F). This effect was also suppressed by 680C91. In the TST, immobility time was increased in DSS-treated mice, and the increase was suppressed by 680C91 (Fig. 6F).

The decreases in locomotor activity in the EPM and OFT observed in the DSS-treated mice may affect anxiodepressive-behaviors. As the behavioral test not reflecting motor deficit, the sucrose preference test was performed (Schintu et al., 2012; Caudal et al., 2015). This test has
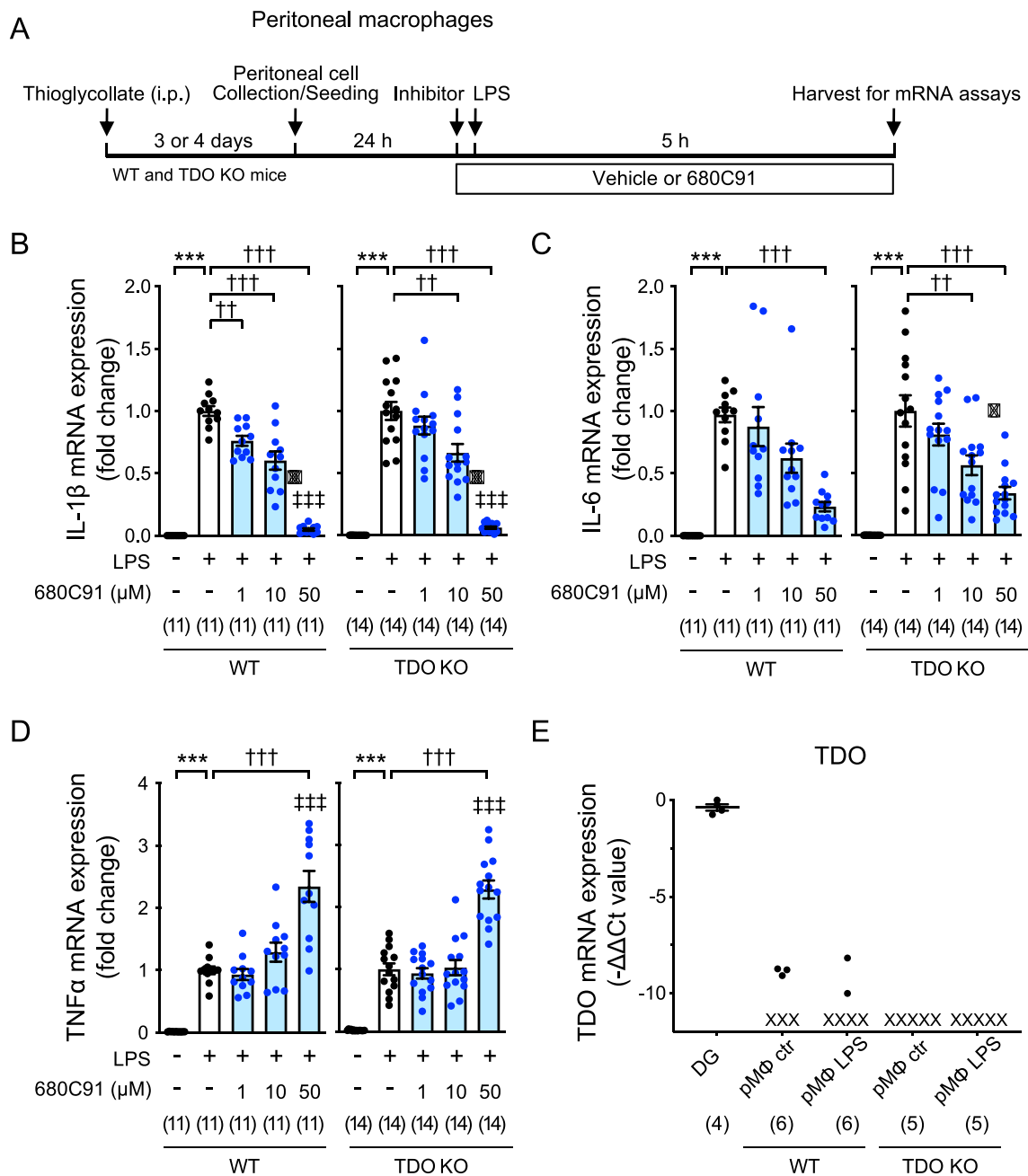
Fig. 3. Effects of 680C91 on the expression of pro-inflammatory cytokine mRNAs in LPS-stimulated peritoneal macrophages from wild-type and TDO KO mice. (A) Experimental design for preparation of peritoneal macrophages from wild-type (WT) and TDO KO mice and treatment of peritoneal macrophages with LPS and/or 680C91. (B-D) Effects of 680C91 (1, 10, 50 µM) on LPS-induced expression of IL-1β (B), IL-6 (C) and TNFα (D) mRNAs in peritoneal macrophages prepared from wild-type and TDO KO mice. After 30 min of incubation with 680C91, peritoneal macrophages were stimulated with LPS at 100 ng/ml for 5 h in the continuous presence of 680C91. The mRNA levels were normalized to LPS alone. (E) TDO mRNA expression in the hippocampal dentate gyrus (DG) from C57Bl/6J mice and peritoneal macrophages (pMΦ). The TDO mRNA levels are normalized to those in the DG and are expressed as -ΔΔCt values. ×, not detected. Data represent mean ± SEM, and the number of experiments in each group is provided under columns. ***$p < 0.001$ vs. the control group; Student's *t*-test. ††$p < 0.01$, †††$p < 0.001$ vs. the group with LPS alone; ‡‡‡$p < 0.001$ vs. the group with LPS/680C91 (1 µM); §§$p < 0.01$, §§§$p < 0.001$ vs. the group with LPS/680C91 (10 µM); one-way ANOVA and Bonferroni multiple comparison test.

been used as a measure of anhedonia (loss of interest or pleasure in all or almost all activities), which is one of core symptoms of depression and is associated with dysfunction of the mesolimbic dopamine system (Cryan and Mombereau, 2004). The sucrose preference was reduced without affecting the total liquid consumption in the DSS-treated mice, and the reduction was abolished by 680C91 (Fig. 6G, H).

These results demonstrated that DSS-induced colitis caused neuro-behavioral impairments in the recovery phase, when the inflammatory responses had largely subsided which were reversed by 680C91

treatment.

3.7. Dopamine responses to rewarding stimuli in the NAc in the recovery phase of DSS-induced colitis

Immune activation and the release of pro-inflammatory cytokines can preferentially affect the dopamine reward circuitry, resulting in reduced motivation and motor slowing (Felger and Treadway, 2017). We therefore investigated the mesolimbic dopamine neurotransmission
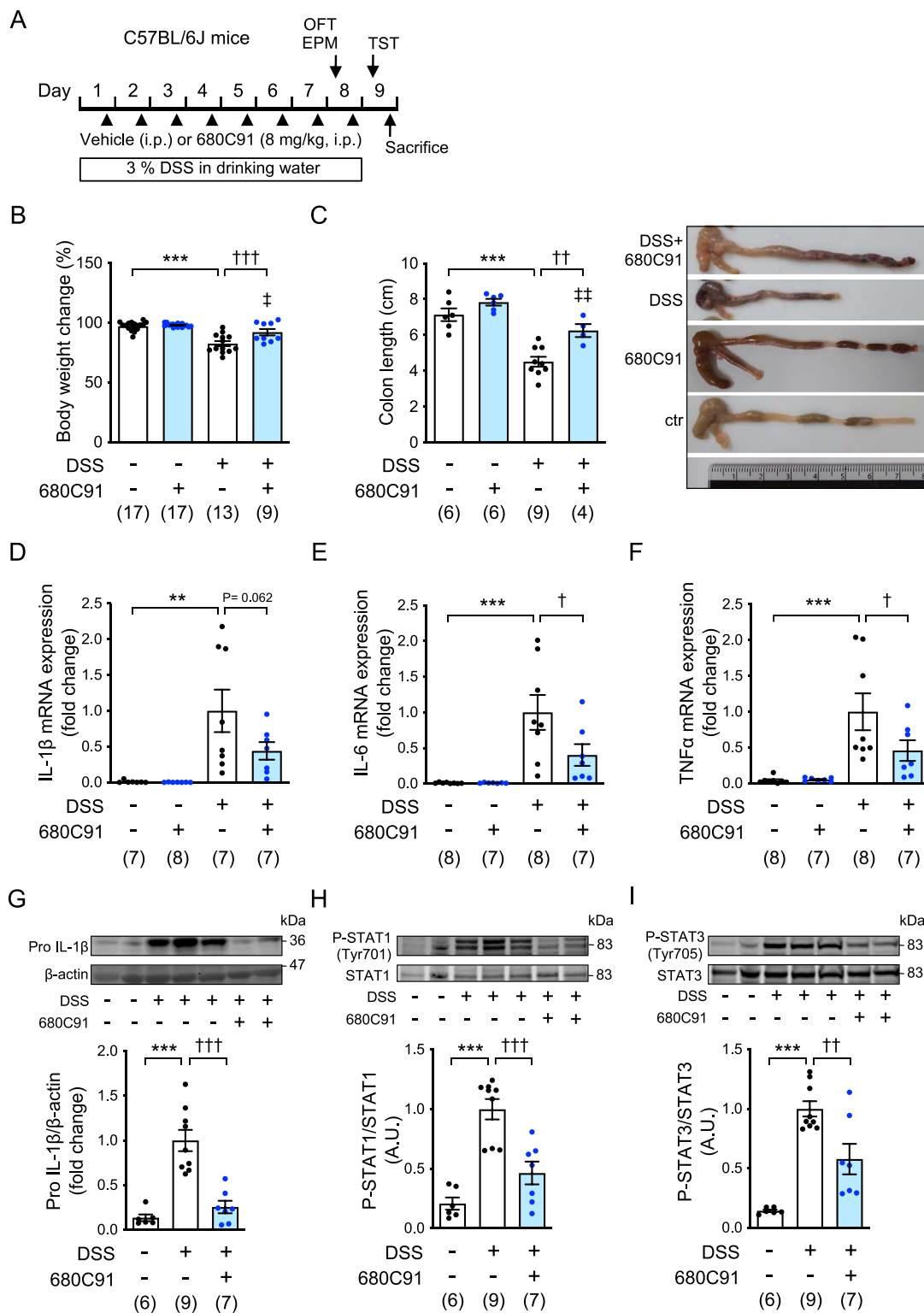
Fig. 4. Effects of 680C91 on the severity of DSS-induced colitis and the inflammatory responses of colon tissues to DSS on Day 9. (A) Experimental design for the acute phase of DSS-induced colitis with 680C91 administration. C57BL/6J mice were assigned randomly to experimental groups, and received 3% DSS in drinking water for 8 days (Day 1–8) and vehicle or 680C91 (8 mg/kg) i.p. injection once a day for 8 days (Day 1–8), as indicated with arrow heads. Behavioral tests were performed on Day 8 (OFT and EPM) and Day 9 (TST), and sacrificed on Day 9 after TST for colon tissue sampling. (B, C) Body weight on Day 9 (percentage of initial body weight on Day 1) (B) and appearance of colon and colon length of mice on Day 9 (C). (D-F) Effects of 680C91 on mRNA levels of IL-1β (D), IL-6 (E) and TNFα (F) in colon tissues in the acute phase of DSS-induced colitis. mRNA levels were normalized to the group with DSS alone. (G-K) Effects of 680C91 on the protein levels of pro-IL-1β (G, H) and the phosphorylation of STAT1 at Tyr701 (I, J) and STAT3 at Tyr705 (I, K) in colon tissues in the acute phase of DSS-induced colitis. Typical blots are shown in (G, I) with quantitation (H, J, K). The protein levels of pro-IL-1β were normalized to β-actin and the group with DSS alone, and p-STAT1 and p-STAT3 were normalized to the corresponding total proteins and the group with DSS alone. Data represent mean ± SEM, and the number of experiments in each group is provided under columns. **$p < 0.01$, ***$p < 0.001$ vs. the control group; †$p < 0.05$, ††$p < 0.01$, †††$p < 0.001$ vs. the group with DSS alone; ‡$p < 0.05$, ‡‡$p < 0.01$ vs. the group with 680C91 alone; one-way ANOVA (C, H, J, K) or two-way ANOVA (A, D-F) and Bonferroni multiple comparison test.
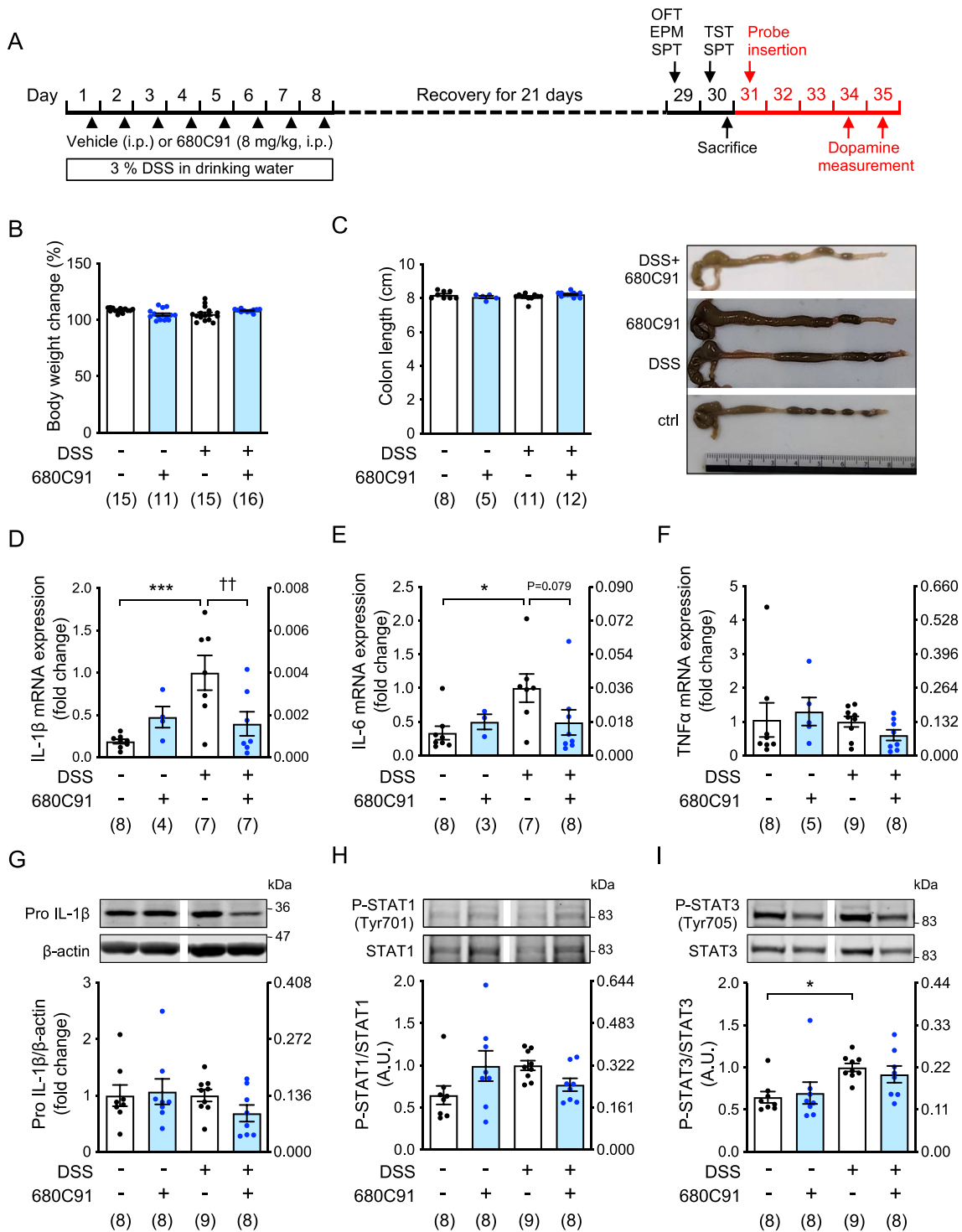
Fig. 5. Effects of 680C91 on DSS-induced colitis and inflammation in the recovery phase (Day 29 and 30). (A) Experimental design for the recovery phase of DSS-induced colitis with 680C91 administration. Mice were assigned randomly to experimental groups, and received 3% DSS in drinking water for 8 days (Day 1–8) and vehicle or 680C91 (8 mg/kg) i.p. injection once a day for 8 days (Day 1–8; arrow heads), as shown in Fig. 4A. After 21 days of recovery time, behavioral tests were performed on Day 29 (OFT and EPM) and Day 30 (TST), and sacrificed on Day 30 after TST for colon tissue sampling. (B, C) Body weight (percentage of initial body weight on Day 1) (B) and appearance of colon and colon length (C) on Day 30. (D-F) Effects of 680C91 on mRNA levels of IL-1β (D), IL-6 (E) and TNFα (F) in colon tissues in the recovery phase of DSS-induced colitis. mRNA levels were normalized to the group with DSS alone. (G-I) Effects of 680C91 on the protein levels of pro-IL-1β (G) and the phosphorylation of STAT1 (H) and STAT3 (I) in colon tissues in the recovery phase of DSS-induced colitis. Typical images of Western blotting are shown with quantitation. The protein levels of pro-IL-1β were normalized to β-actin and the group with DSS alone, and pSTAT1 and pSTAT3 were normalized to the corresponding total proteins and the group with DSS alone. The right axis of (D-I) indicates the relative values of the corresponding groups with DSS alone on Day 9 (Fig. 4D-F, H, J, K). Data represent mean $\pm$ SEM, and the number of experiments in each group is provided under columns. *$p < 0.05$, ***$p < 0.001$ vs. the control group; $^{\dagger\dagger}p < 0.01$ vs. the group with DSS alone; two-way ANOVA and Bonferroni multiple comparison test.
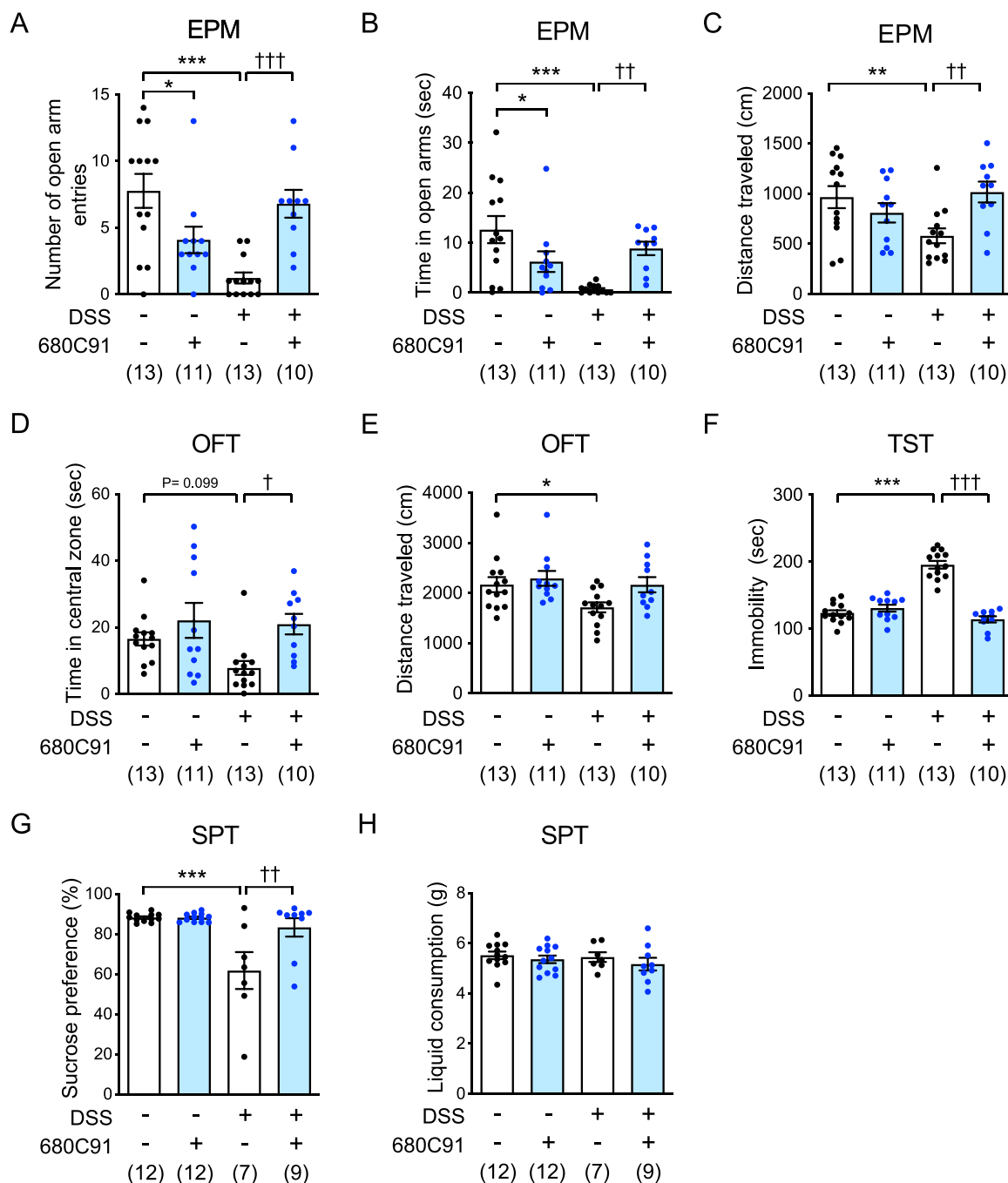
Fig. 6. Impaired neurobehaviors during the recovery phase of DSS-induced colitis are reversed by 680C91. Neurobehavioral effects were evaluated with the EPM (A-C), OFT (D, E), TST (F) and SPT (G, H). DSS and 680C91 were administered as shown in Fig. 5A, and behavioral tests were performed on Day 29 (EPM, OFT) and Day 30 (TST) after 21 days of recovery time. In the SPT, sucrose preference was measured on Day 29 and 30 using different sets of mice. Data represent mean ± SEM, and the number of experiments in each group is provided under columns. *$p < 0.05$, **$p < 0.01$, ***$p < 0.001$ vs. the control group; †$p < 0.05$, ††$p < 0.01$, †††$p < 0.001$ vs. the group with DSS alone; two-way ANOVA and Bonferroni multiple comparison test.

in DSS and/or 680C91-treated mice in the recovery phase after behavioral tests (Day 34–35). For this purpose, the extracellular levels of dopamine in the NAc in response to a drug of abuse, cocaine, and natural rewarding stimuli, a palatable food or female mouse, were determined with *in vivo* microdialysis. The basal extracellular levels of dopamine were not affected by DSS and/or 680C91 administration (Fig. 7A). In the DSS-treated group (DSS+/680C91−), the increase in the dopamine levels in response to cocaine infusion (1 μM) into the NAc was attenuated compared with the control group (DSS−/680C91−) (Fig. 7B). When 680C91 were administered during DSS administration period (DSS+/680C91 +), the dopamine levels in response to NAc cocaine infusion

were enhanced beyond the levels in the control group. Dopamine response to palatable food in the DSS-treated group was attenuated compared with that in the control group, and 680C91 administration reversed the attenuated dopamine response in the DSS-treated group (Fig. 7C). Similar to palatable food, dopamine response to the exposure to a female mouse was attenuated by DSS administration, and the attenuated response was reversed by 680C91 administration (Fig. 7D). These results suggest that DSS-induced colitis attenuates the dopamine responses to cocaine and natural rewarding stimuli in the NAc, and 680C91 reverses the attenuated dopamine responses. The restoration of dopamine response may be associated with the improvement of
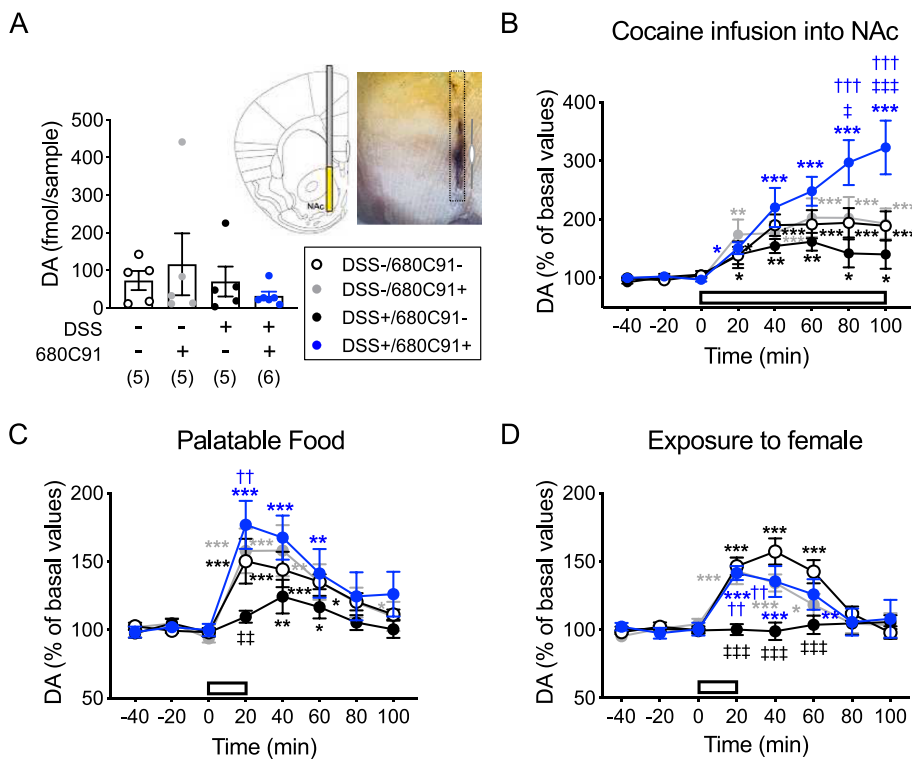
Fig. 7. Negative effects of DSS-induced colitis on dopamine responses to rewarding stimuli in the NAc are reversed by 680C91. (A) The basal extracellular levels of dopamine determined by *in vivo* microdialysis and representative location of a microdialysis probe placed in the NAc on Day 34–35 (see Fig. 5A). Each dot indicates DA values (fmol/sample) expressed as the average of three stable baseline samples in each animal. (B-D) The dopamine (DA) responses to rewarding stimuli in the NAc. The effects of cocaine infusion (1 μM) into the NAc (B), exposure to palatable food (C), and exposure to female mice (D) on the extracellular levels of dopamine in the NAc in mice treated with DSS and/or 680C91. Mice were first exposed to female mice and then exposed to palatable food on Day 34, and cocaine was infused on Day 35. The basal values for each group were obtained as the average of three stable baseline samples, and all values are calculated as a percentage of the basal values within the same group (100%). Data represent mean ± SEM, and the number of mice is indicated under each experimental group. *$p < 0.05$, **$p < 0.01$, ***$p < 0.001$ vs. the basal values within the same group; mixed linear models. $^{†††}p < 0.001$ vs. the group with DSS alone; $^{‡}p < 0.05$, $^{‡‡}p < 0.01$, $^{‡‡‡}p < 0.001$ vs. the control group; two-way ANOVA and Sidak's multiple comparisons test.

anxiodepressive-like behaviors by 680C91.

4. Discussion

We demonstrated that 680C91, which is known as a TDO inhibitor, inhibited LPS-induced production of pro-inflammatory cytokines (IL-1β and IL-6) in a macrophage-like cell line, Raw 264.7 cells and primary peritoneal macrophages. 680C91 suppressed the inflammatory responses via TDO-independent mechanisms, because Raw 264.7 cells expressed very low levels of TDO mRNA and peritoneal macrophages were prepared from TDO KO mice. The anti-inflammatory effects of 680C91 were mediated through the suppression of STAT signaling. Under *in vivo* conditions, 680C91 suppressed the inflammatory responses and STAT signaling in the acute phase of DSS-induced colitis. Studies using TDO KO mice revealed that the anti-inflammatory effects of 680C91 *in vivo* were TDO-independent. Anxiodepressive-like behaviors were observed in the recovery phase of DSS-induced colitis, and the development of anxiodepressive-like behaviors were prevented by 680C91 administered during the acute phase. The role of 680C91 for the prevention of anxiodepressive-like behaviors may be in part explained by the rescue of the attenuated dopamine responses to rewarding stimuli in the NAc. These observations suggest that 680C91 is a novel class of therapeutic agent, which inhibits acute inflammatory responses via STAT-mediated, but TDO-independent mechanisms, and has ability to prevent the development of anxiodepressive-like behaviors in DSS-induced colitis.

4.1. Inhibition of inflammatory responses to LPS by 680C91

LPS is known to activate macrophages via TLR4-mediated signaling and induces the production of pro-inflammatory cytokines, leading to the development of systemic inflammation (Akira et al., 2006; Qureshi et al., 2012; Bessede et al., 2014). In this study, LPS induced the production of pro-inflammatory cytokines in Raw 264.7 cells and peritoneal macrophages, and the production of cytokines was suppressed by 680C91. 680C91 at 10 μM used in this study selectively inhibits TDO

without inhibitory activity against IDO1 in cells (Salter et al., 1995; Pilotte et al., 2012). In fact, 680C91 at 10 μM inhibited the conversion of tryptophan to kynurenine by TDO in THP-1 cells. Interestingly, the effects of 680C91 to suppress the cytokine production were not mediated through TDO inhibition because the expression of TDO in Raw 264.7 cells and peritoneal macrophages from wild-type mice was very low. Furthermore, 680C91 showed the suppression of cytokine production in peritoneal macrophages from TDO KO mice. It is unlikely that the suppression of the cytokine production by 680C91 is mediated through IDO inhibition as the IDO1 inhibitor failed to induce similar effects or through inhibition of compensatory TDO-like activity in peritoneal macrophages from TDO KO mice as another TDO inhibitor failed.

The molecular mechanisms by which 680C91 suppresses LPS-induced production of proinflammatory cytokines are not elucidated in this study. Surprisingly, another TDO inhibitor, LM10, did not show the ability to suppress the cytokine production. LM10 is structurally related to 680C91: 6-fluolo-indole with replacement of 3-pyridyl side chain in the 3-position by tetrazole side chain (Dolušić et al., 2011; Pilotte et al., 2012). Although 3-pyridyl side chain is reported to stabilize 680C91 within the TDO binding cleft (Dolušić et al., 2011), 3-pyridyl side chain may play a critical role in the anti-inflammatory action of 680C91.

Binding of LPS to TLR4 has been shown to induce activation of the MyD88-dependent and Toll/IL-1R homology domain-containing adaptor protein inducing IFNβ (TRIF) -dependent signaling pathways, leading to activation of the MAP kinase, NF-κB and IRF3 cascades (Akira et al., 2006; Qin et al., 2016). Activation of theses signaling pathways results in the induction of proinflammatory cytokines and type I IFNs. Subsequent induction of IFNβ activates JAK-STAT signaling via the IFN α/β receptor (Fujihara et al., 2003; Bode et al., 2012). In fact, LPS has been shown to activate STAT1 and STAT3 in macrophage (Samavati et al., 2009). In this study, the effects of 680C91 on downstream signaling molecules of LPS/TLR4 were screened in Raw 264.7 cells, and we found that the LPS-stimulated phosphorylation of STAT1 and STAT3 was downregulated by 680C91, suggesting that 680C91 may interact with signaling molecules of the JAK-STAT pathway.

It has been shown that the JAK2-STAT1/3 signaling pathway plays critical roles in the induction of IL-1β and IL-6 via activation of a STAT binding element in the promoter regions, which is conserved in IL-1β and IL-6 genes, but not in TNFα gene (Lee et al., 2006). Furthermore, the inhibition of STAT3 is shown to attenuate the LPS-induced expression of IL-1β and IL-6, but not of TNFα, in Raw 264.7 cells (Samavati et al., 2009). The role of STAT3 in IL-6 induction is reported in cancer cells. STAT3 is activated by cytokine receptor/JAK signaling and the phosphorylated STAT3 translocates to the nucleus and cooperates with NF-κB to produce IL-6, resulting in the induction of cancer-associated inflammation (Yoon et al., 2012; Tzeng et al., 2021). Interestingly, mollugin, a JAK2 inhibitor isolated from Rubia cordifolia L., attenuates the LPS-induced expression of IL-1β and IL-6, but enhances the expression of TNFα in Raw 264.7 cells (Zhu et al., 2013), which pattern resembles to that of 680C91, although the mechanisms for the enhanced expression of TNFα are unknown. These findings support the hypothesis that 680C91 may act as an inhibitor of the JAK-STAT pathway, leading to the suppression of IL-1β and IL-6 expression.

4.2. Inhibition of inflammatory responses in DSS-induced colitis by 680C91

DSS-induced colitis is an animal model of IBD (Perše and Cerar, 2012). DSS induces the production of macrophage-derived cytokines such as IL-1β, IL-6, and TNFα (Dieleman et al., 1994), and the cytokine profiles correlate with clinical and histological parameters of DSS-induced colitis (Perše and Cerar, 2012). In this study, 3% DSS in drinking water for 8 days induced the inflammation of colon and the production of IL-1β, IL-6, and TNFα in the acute phase (Day 9), and the inflammatory responses subsided close to control levels in the recovery phase (Day 30). The inflammatory responses in the acute phase were largely attenuated by 680C91 via TDO-independent mechanisms, and the effects of 680C91 were retained until the recovery phase. The inhibition of the inflammatory responses by 680C91 is presumably mediated through action on intestinal macrophages. Intestinal macrophages are known to play critical roles in intestinal inflammation and resolution of IBD (de Souza and Fiocchi, 2016; Na et al., 2019). In the inflammatory phase of IBD, the shift of macrophage from mature to immature macrophage is induced by infiltrating neutrophils and recruited inflammatory monocytes, leading to the production of inflammatory cytokines that promote type 1 helper T (T$_H$1) cell and T$_H$17 cell immune responses towards invading organisms and epithelial cells (Na et al., 2019), although immature macrophage switches to resolving macrophage to repair damaged epithelium in the resolution phase. The ability of 680C91 to inhibit cytokine production in macrophage may be effective to suppress the inflammatory propagation in IBD.

In the IBD, the JAK-STAT signaling pathway mediates biological effects of proinflammatory cytokines including activation of B cells and differentiation of naïve helper T (Th0) cells (Coskun et al., 2013; Salas et al., 2020). The JAK-STAT signaling pathway serves as a therapeutic target of IBD, and JAK inhibitors such as tofacitinib have the potential to inhibit cytokine-dependent pathways involved in IBD pathogenesis (Salas et al., 2020). In DSS-induced colitis, STAT1/3 signaling in colon tissues was activated in the acute phase, as previously reported (Kim et al., 2019). 680C91 was able to suppress activation of STAT1/3 signaling in DSS-induced colitis as well as cultured macrophages. The ability of 680C91 to inhibit JAK-STAT1/3 signaling may exert anti-inflammatory effects in the treatment of IBD.

4.3. Anxiodepressive-like behaviors in DSS-induced colitis

In animal models of IBD, comorbid depression-like behaviors have been reported (Bercik et al., 2011; Chen et al., 2015; Abautret-Daly et al., 2018). In this study, mice with DSS-induced colitis exhibited anxiodepressive-like behaviors in the acute and recovery phases. Several previous reports demonstrated anxiodepressive-like behaviors in the acute phase of DSS-induced colitis (Chen et al., 2015; Abautret-Daly et al., 2018; Nakagawasai et al., 2020). However, in the acute phase, mice were suffered from abdominal pain and diarrhea due to active bowel inflammation, and therefore some of the behavioral changes can be classified as sickness behavior, an adaptive response to sickness (Abautret-Daly et al., 2018). We could detect anxiodepressive-like behaviors in the recovery phase of DSS-induced colitis, after 21 days of recovery. Along the same lines, anxiodepressive-like behaviors including anhedonia were observed in the early recovery phase (after ~8 days of recovery) of DSS-induced colitis (Dempsey et al., 2019), but the normalization of the impaired recognition memory and anxiety in the early recovery phase (after 9 days of recovery) was also reported (Emge et al., 2016). The reason for the different persistency of anxiodepressive-like behaviors is currently unknown, but the strength of DSS-induced colitis and environmental factors such as stress may be factors affecting the persistency. In addition, a limitation of this study is the use of only male mice, and sex differences of anxiodepressive-like behaviors in response to DSS-induced colitis need to be examined in future studies.

Anxiodepressive-like behaviors in the recovery phase are not likely mediated through active bowel inflammation, because the inflammatory responses to DSS subsided close to the control levels by Day 30. 680C91 treatment during DSS administration suppressed the development of anxiodepressive-like behaviors, presumably because 680C91 attenuated the production of inflammatory cytokines in the acute phase, resulting in the reduced priming of brain for cytokine-induced depression. Besides the TDO-independent inhibition of JAK-STAT signaling and subsequent cytokine production by 680C91, 680C91 is supposed to act as a TDO inhibitor *in vivo* as observed in THP-1-derived macrophages. The tryptophan-kynurenine pathway is known to mediate gut-brain interaction underlying comorbid depression with IBD (Chen et al., 2021). 680C91 administration has been shown to increase brain levels of tryptophan and 5-HT in rats (Salter et al., 1995), and it is possible that upregulation of 5-HT signaling by 680C91-mediated TDO inhibition in the acute phase of DSS-induced colitis contributes to the suppression of anxiodepressive-like behaviors. In IBD, overactivation of IDO, but not TDO, by intestinal inflammation results in the conversion of tryptophan to kynurenine, and the increased production of kynurenine and its metabolites especially quinolinic acid cause depression by damaging neurons (Chen et al., 2021). Therefore, the contribution of 680C91 as a TDO inhibitor to the suppression of anxiodepressive-like behaviors may be limited in DSS-induced colitis. Future studies to evaluate the effects of 680C91 on kynurenine and 5-HT metabolites in mouse brain with DSS-induced colitis are required.

Neural mechanisms of depression associated with IBD have been studied in animal models of IBD including DSS-induced colitis (Abautret-Daly et al., 2018). Intestinal inflammation induces the increased permeability of blood brain barrier, central inflammation and activation of the hypothalamus–pituitary–adrenal axis (Abautret-Daly et al., 2018). In mice with DSS-induced colitis, the increase in proinflammatory cytokines in several brain regions (Takahashi et al., 2019; Zhao et al., 2020; Dong et al., 2021), the suppression of BDNF and neurogenesis in the hippocampus (Takahashi et al., 2019; Nakagawasai et al., 2020; Zhao et al., 2020), and activation of astrocytes and microglia (Nakagawasai et al., 2020; Dong et al., 2021) have been reported. Proinflammatory cytokines such as IL-1β can penetrate the blood–brain barrier into brain regions, resulting in the induction of depression-like behaviors (Yang et al., 2023). Alternatively, proinflammatory cytokines are produced by neurons and non-neuronal cells including astrocytes and microglia (Yang et al., 2023), suggesting that 680C91 acting in the brain may inhibit inflammatory responses of neurons. However, the role of 680C91 to inhibit the production of proinflammatory cytokines in the brain seems to be limited, because the expression of cytokine mRNAs in the NAc screened with RNA-seq analyses were not altered during acute and recovery phases of DSS-induced colitis (Kuroiwa M and Nishi A, unpublished observations).

The JAK-STAT pathway is involved in the regulation of neural functions including neurogenesis, synaptic plasticity, gliogenesis and microglial activation, which are implicated in pathogenesis of depression (Shariq et al., 2018; Borbély et al., 2022). The inhibition of JAK3 is shown to restore the stress-induced attenuation of neurogenesis and depression-like behaviors in mice (Gulbins et al., 2016). JAK inhibitors are now used for the treatment of inflammatory disorders including rheumatoid arthritis and IBD, and indirect clinical data suggest that JAK inhibitors significantly improve mood (Panés et al., 2015; Schiff et al., 2017). Therefore, JAK-STAT inhibitors are proposed as therapeutic options of depression (Shariq et al., 2018; Borbély et al., 2022), and 680C91 is expected to exert antidepressant action by modulating the JAK-STAT pathways in inflammatory disorders.

Peripheral inflammation and the released cytokines affect the synthesis and release of dopamine and dopamine receptor signaling, leading to the suppression of dopamine neurotransmission, which are associated with the impaired motivation and motor activity (Felger and Treadway, 2017). We demonstrated that dopamine responses to rewarding stimuli were attenuated in the NAc in mice with DSS-induced colitis in the recovery phase. In line with our results, DSS-induced colitis is shown to exacerbate the degeneration of dopamine neurons in an animal model of Parkinson's disease (Villarán et al., 2010). The dysfunction of dopamine neurotransmission may be one of neural mechanisms for anxiodepressive-like behaviors in DSS-induced colitis. In fact, anhedonia, which is associated with the dysfunction of mesolimbic dopamine system (Cryan and Mombereau, 2004), was present in mice with DSS-induced colitis. 680C91 administration during acute phase of DSS-induced colitis was able to prevent the dysfunction of dopamine neurotransmission and the development of anhedonia. Thus, the use of 680C91 in the acute phase of inflammation may be effective in suppressing inflammatory propagation, and may prevent the development of anxiety and depression in inflammatory disorders.

5. Conclusion

We demonstrated that 680C91 known as the TDO inhibitor shows anti-inflammatory properties in cultured macrophages and mice with DSS-induced colitis, while reversing comorbid neurobehavioral maladaptations. 680C91 exhibited TDO-independent effects which may contribute to its ability to attenuate gastrointestinal inflammation and neurobehavioral impairments. Future identification of molecular mechanisms for anti-inflammatory action of 680C91 may contribute to the develop a novel class of anti-inflammatory drugs.

Declaration of Competing Interest

The authors declare that they have no known competing financial interests or personal relationships that could have appeared to influence the work reported in this paper.

Data availability

No data was used for the research described in the article.

Acknowledgements

Appendix A. Supplementary data

Supplementary data to this article can be found online at https://doi. org/10.1016/j.bbi.2023.08.019.

References

Abautret-Daly, Á., Dempsey, E., Parra-Blanco, A., Medina, C., Harkin, A., 2018. Gut-brain actions underlying comorbid anxiety and depression associated with inflammatory bowel disease. Acta Neuropsychiatr 30 (5), 275–296.

Abuin-Martínez, C., Vidal, R., Gutiérrez-López, M.D., Pérez-Hernández, M., Giménez-Gómez, P., Morales-Puerto, N., O'Shea, E., Colado, M.I., 2021. Increased kynurenine concentration attenuates serotonergic neurotoxicity induced by 3,4-methylenedioxymethamphetamine (MDMA) in rats through activation of aryl hydrocarbon receptor. Neuropharmacology 187, 108490.

Akira, S., Uematsu, S., Takeuchi, O., 2006. Pathogen recognition and innate immunity. Cell 124 (4), 783–801.

Ala, M., 2021. The footprint of kynurenine pathway in every cancer: a new target for chemotherapy. Eur. J. Pharmacol. 896, 173921.

Barberio, B., Zamani, M., Black, C.J., Savarino, E.V., Ford, A.C., 2021. Prevalence of symptoms of anxiety and depression in patients with inflammatory bowel disease: a systematic review and meta-analysis. Lancet Gastroenterol. Hepatol. 6 (5), 359–370.

Baumgartner, R., Forteza, M.J., Ketelhuth, D.F.J., 2019. The interplay between cytokines and the Kynurenine pathway in inflammation and atherosclerosis. Cytokine 122, 154148.

Bercik, P., Park, A.J., Sinclair, D., Khoshdel, A., Lu, J., Huang, X., Deng, Y., Blennerhassett, P.A., Fahnestock, M., Moine, D., Berger, B., Huizinga, J.D., Kunze, W., McLean, P.G., Bergonzelli, G.E., Collins, S.M., Verdu, E.F., 2011. The anxiolytic effect of Bifidobacterium longum NCC3001 involves vagal pathways for gut-brain communication. Neurogastroenterol. Motil. 23, 1132–1139.

Bessede, A., Gargaro, M., Pallotta, M.T., Matino, D., Servillo, G., Brunacci, C., Bicciato, S., Mazza, E.M.C., Macchiarulo, A., Vacca, C., Iannitti, R., Tissi, L., Volpi, C., Belladonna, M.L., Orabona, C., Bianchi, R., Lanz, T.V., Platten, M., Della Fazia, M.A., Piobbico, D., Zelante, T., Funakoshi, H., Nakamura, T., Gilot, D., Denison, M.S., Guillemin, G.J., DuHadaway, J.B., Prendergast, G.C., Metz, R., Geffard, M., Boon, L., Pirro, M., Iorio, A., Veyret, B., Romani, L., Grohmann, U., Fallarino, F., Puccetti, P., 2014. Aryl hydrocarbon receptor control of a disease tolerance defence pathway. Nature 511 (7508), 184–190.

Beurel, E., Toups, M., Nemeroff, C.B., 2020. The Bidirectional Relationship of Depression and Inflammation: Double Trouble. Neuron 107 (2), 234–256.

Bode, J.G., Ehlting, C., Häussinger, D., 2012. The macrophage response towards LPS and its control through the p38(MAPK)-STAT3 axis. Cell. Signal. 24 (6), 1185–1194.

Borbély, É., Simon, M., Fuchs, E., Wiborg, O., Czéh, B., Helyes, Z., 2022. Novel drug developmental strategies for treatment-resistant depression. Br. J. Pharmacol. 179 (6), 1146–1186.

Caudal, D., Alvarsson, A., Björklund, A., Svenningsson, P., 2015. Depressive-like phenotype induced by AAV-mediated overexpression of human α-synuclein in midbrain dopaminergic neurons. Exp. Neurol. 273, 243–252.

Cervenka, I., Agudelo, L.Z., Ruas, J.L., 2017. Kynurenines: Tryptophan's metabolites in exercise, inflammation, and mental health. Science 357 (6349).

Chassaing, B., Aitken, J.D., Malleshappa, M., Vijay-Kumar, M., 2014. Dextran sulfate sodium (DSS)-induced colitis in mice. Curr. Protoc. Immunol. 104 (1).

Chen, L.M., Bao, C.H., Wu, Y., Liang, S.H., Wang, D., Wu, L.Y., Huang, Y., Liu, H.R., Wu, H.G., 2021. Tryptophan-kynurenine metabolism: a link between the gut and brain for depression in inflammatory bowel disease. J. Neuroinflammation 18, 135.

Chen, Y., Guillemin, G.J., 2009. Kynurenine pathway metabolites in humans: disease and healthy States. Int J Tryptophan Res 2, 1–19.

Chen, J., Winston, J.H., Fu, Y.u., Guptarak, J., Jensen, K.L., Shi, X.-Z., Green, T.A., Sarna, S.K., 2015. Genesis of anxiety, depression, and ongoing abdominal discomfort in ulcerative colitis-like colon inflammation. Am. J. Physiol. Regul. Integr. Comp. Physiol. 308 (1), R18–R27.

Cheong, J.E., Sun, L., 2018. Targeting the IDO1/TDO2-KYN-AhR Pathway for Cancer Immunotherapy - Challenges and Opportunities. Trends Pharmacol. Sci. 39 (3), 307–325.

Coskun, M., Salem, M., Pedersen, J., Nielsen, O.H., 2013. Involvement of JAK/STAT signaling in the pathogenesis of inflammatory bowel disease. Pharmacol. Res. 76, 1–8.

Cryan, J.F., Mombereau, C., 2004. In search of a depressed mouse: utility of models for studying depression-related behavior in genetically modified mice. Mol. Psychiatry 9 (4), 326–357.

de Souza, H.S.P., Fiocchi, C., 2016. Immunopathogenesis of IBD: current state of the art. Nat. Rev. Gastroenterol. Hepatol. 13 (1), 13–27.

Dempsey, E., Abautret-Daly, Á., Docherty, N.G., Medina, C., Harkin, A., 2019. Persistent central inflammation and region specific cellular activation accompany depression- and anxiety-like behaviours during the resolution phase of experimental colitis. Brain Behav. Immun. 80, 616–632.

Dieleman, L.A., Ridwan, B.U., Tennyson, G.S., Beagley, K.W., Bucy, R.P., Elson, C.O., 1994. Dextran sulfate sodium-induced colitis occurs in severe combined immunodeficient mice. Gastroenterology 107 (6), 1643–1652.

Dolušić, E., Larrieu, P., Moineaux, L., Stroobant, V., Pilotte, L., Colau, D., Pochet, L., Van den Eynde, B., Masereel, B., Wouters, J., Frédérick, R., 2011. Tryptophan 2,3-dioxygenase (TDO) inhibitors. 3-(2-(pyridyl)ethenyl)indoles as potential anticancer immunomodulators. J. Med. Chem. 54 (15), 5320–5334.

Dong, X., Lu, H., Lin, P., Che, H., Li, H., Song, L., Yang, X., Xie, W., 2021. Saccharina japonica Ethanol Extract Ameliorates Depression/Anxiety-Like Behavior by Inhibiting Inflammation, Oxidative Stress, and Apoptosis in Dextran Sodium Sulfate Induced Ulcerative Colitis Mice. Front. Nutr. 8, 784532.

Emge, J.R., Huynh, K., Miller, E.N., Kaur, M., Reardon, C., Barrett, K.E., Gareau, M.G., 2016. Modulation of the microbiota-gut-brain axis by probiotics in a murine model of inflammatory bowel disease. Am. J. Physiol. Gastrointest. Liver Physiol. 310 (11), G989–G998.

Felger, J.C., Treadway, M.T., 2017. Inflammation Effects on Motivation and Motor Activity: Role of Dopamine. Neuropsychopharmacology 42 (1), 216–241.

Fox, E., Oliver, T., Rowe, M., Thomas, S., Zakharia, Y., Gilman, P.B., Muller, A.J., Prendergast, G.C., 2018. Indoximod: An Immunometabolic Adjuvant That Empowers T Cell Activity in Cancer. Front. Oncol. 8, 370.

Fujigaki, H., Saito, K., Fujigaki, S., Takemura, M., Sudo, K., Ishiguro, H., Seishima, M., 2006. The signal transducer and activator of transcription 1alpha and interferon regulatory factor 1 are not essential for the induction of indoleamine 2,3-dioxygenase by lipopolysaccharide: involvement of p38 mitogen-activated protein kinase and nuclear factor-kappaB pathways, and synergistic effect of several proinflammatory cytokines. J. Biochem. 139, 655–662.

Fujihara, M., Muroi, M., Tanamoto, K.-I., Suzuki, T., Azuma, H., Ikeda, H., 2003. Molecular mechanisms of macrophage activation and deactivation by lipopolysaccharide: roles of the receptor complex. Pharmacol. Ther. 100 (2), 171–194.

Gulbins, A., Grassmé, H., Hoehn, R., Kohnen, M., Edwards, M.J., Kornhuber, J., Gulbins, E., 2016. Role of Janus-Kinases in Major Depressive Disorder. Neurosignals 24, 71–80.

Hanada, Y., Kawahara, Y., Ohnishi, Y.N., Shuto, T., Kuroiwa, M., Sotogaku, N., Greengard, P., Sagi, Y., Nishi, A., 2018. Cholinergic Interneurons of the Nucleus Accumbens Is Essential for Dopamine Responses to Rewarding Stimuli. eNeuro 5 (5). ENEURO.0332-18.2018.

Hattori, S., Takao, K., Funakoshi, H., Miyakawa, T., 2018. Comprehensive behavioral analysis of tryptophan 2,3-dioxygenase (Tdo2) knockout mice. Neuropsychopharmacol Rep 38 (2), 52–60.

Hoffmann, D., Pilotte, L., Stroobant, V., Van den Eynde, B.J., 2019. Induction of tryptophan 2,3-dioxygenase expression in human monocytic leukemia/lymphoma cell lines THP-1 and U937. Int J Tryptophan Res 12, 1178646919891736.

Howren, M.B., Lamkin, D.M., Suls, J., 2009. Associations of depression with C-reactive protein, IL-1, and IL-6: a meta-analysis. Psychosom. Med. 71, 171–186.

Kanai, M., Funakoshi, H., Takahashi, H., Hayakawa, T., Mizuno, S., Matsumoto, K., Nakamura, T., 2009. Tryptophan 2,3-dioxygenase is a key modulator of physiological neurogenesis and anxiety-related behavior in mice. Mol. Brain 2, 8.

Kawahara, Y., Kaneko, F., Yamada, M., Kishikawa, Y., Kawahara, H., Nishi, A., 2013. Food reward-sensitive interaction of ghrelin and opioid receptor pathways in mesolimbic dopamine system. Neuropharmacology 67, 395–402.

Kim, T.W., Shin, J.S., Chung, K.S., Lee, Y.G., Baek, N.I., Lee, K.T., 2019. Anti-Inflammatory Mechanisms of Koreanaside A, a Lignan Isolated from the Flower of Forsythia koreana, against LPS-Induced Macrophage Activation and DSS-Induced Colitis Mice: The Crucial Role of AP-1, NF-κB, and JAK/STAT Signaling. Cells 8.

Kim, M., Tomek, P., 2021. Tryptophan: A Rheostat of Cancer Immune Escape Mediated by Immunosuppressive Enzymes IDO1 and TDO. Front. Immunol. 12, 636081.

Koga, M., Yamauchi, A., Kanaoka, Y., Jige, R., Tsukamoto, A., Teshima, N., Nishioku, T., Kataoka, Y., 2013. BMP4 is increased in the aortas of diabetic ApoE knockout mice and enhances uptake of oxidized low density lipoprotein into peritoneal macrophages. J. Inflamm. (Lond.) 10, 32.

Köhler, C.A., Freitas, T.H., Maes, M., de Andrade, N.Q., Liu, C.S., Fernandes, B.S., Stubbs, B., Solmi, M., Veronese, N., Herrmann, N., Raison, C.L., Miller, B.J., Lanctôt, K.L., Carvalho, A.F., 2017. Peripheral cytokine and chemokine alterations in depression: a meta-analysis of 82 studies. Acta Psychiatr. Scand. 135 (5), 373–387.

Lee, C., Lim, H.K., Sakong, J., Lee, Y.S., Kim, J.R., Baek, S.H., 2006. Janus kinase-signal transducer and activator of transcription mediates phosphatidic acid-induced interleukin (IL)-1beta and IL-6 production. Mol. Pharmacol. 69, 1041–1047.

Maes, M., Leonard, B.E., Myint, A.M., Kubera, M., Verkerk, R., 2011. The new '5-HT' hypothesis of depression: cell-mediated immune activation induces indoleamine 2,3-dioxygenase, which leads to lower plasma tryptophan and an increased synthesis of detrimental tryptophan catabolites (TRYCATs), both of which contribute to the onset of depression. Prog. Neuropsychopharmacol. Biol. Psychiatry 35 (3), 702–721.

Modoux, M., Rolhion, N., Mani, S., Sokol, H., 2021. Tryptophan Metabolism as a Pharmacological Target. Trends Pharmacol. Sci. 42 (1), 60–73.

Murakami, Y., Imamura, Y., Kasahara, Y., Yoshida, C., Momono, Y., Fang, K., Nishiyama, T., Sakai, D., Konishi, Y., 2021. The Effects of Maternal Interleukin-17A on Social Behavior, Cognitive Function, and Depression-Like Behavior in Mice with Altered Kynurenine Metabolites. Int J Tryptophan Res 14, 1178646921026639.

Na, Y.R., Stakenborg, M., Seok, S.H., Matteoli, G., 2019. Macrophages in intestinal inflammation and resolution: a potential therapeutic target in IBD. Nat. Rev. Gastroenterol. Hepatol. 16 (9), 531–543.

Nakagawasai, O., Yamada, K., Takahashi, K., Odaira, T., Sakuma, W., Ishizawa, D., Takahashi, N., Onuma, K., Hozumi, C., Nemoto, W., Tan-No, K., 2020. Liver hydrolysate prevents depressive-like behavior in an animal model of colitis: Involvement of hippocampal neurogenesis via the AMPK/BDNF pathway. Behav. Brain Res. 390, 112640.

Neuendorf, R., Harding, A., Stello, N., Hanes, D., Wahbeh, H., 2016. Depression and anxiety in patients with Inflammatory Bowel Disease: A systematic review. J. Psychosom. Res. 87, 70–80.

Ohta, Y., Kubo, H., Yashiro, K., Ohashi, K., Tsuzuki, Y., Wada, N., Yamamoto, Y., Saito, K., 2017. Effect of water-immersion restraint stress on tryptophan catabolism through the kynurenine pathway in rat tissues. J. Physiol. Sci. 67 (3), 361–372.

Oldak, B., Cruz-Rivera, M., Flisser, A., Mendlovic, F., 2018. RNA Purity, Real-Time PCR Sensitivity, and Colon Segment Influence mRNA Relative Expression in Murine Dextran Sodium Sulfate Experimental Colitis. J. Biomol. Tech. 29 (3), 61–70.

Panés, J., Su, C., Bushmakin, A.G., Cappelleri, J.C., Mamolo, C., Healey, P., 2015. Randomized trial of tofacitinib in active ulcerative colitis: analysis of efficacy based on patient-reported outcomes. BMC Gastroenterol. 15, 14.

Paxinos, G., Franklin, K.B., 2004. The Mouse Brain in Stereotaxic Coordinates; Compact, 2nd Edition. Academic Press.

Perše, M., Cerar, A., 2012. Dextran sodium sulphate colitis mouse model: traps and tricks. J. Biomed. Biotechnol., 718617

Pilotte, L., Larrieu, P., Stroobant, V., Colau, D., Dolušić, E., Frédérick, R., De Plaen, E., Uyttenhove, C., Wouters, J., Masereel, B., Van den Eynde, B.J., 2012. Reversal of tumoral immune resistance by inhibition of tryptophan 2,3-dioxygenase. PNAS 109 (7), 2497–2502.

Qin, X., Jiang, X., Jiang, X., Wang, Y., Miao, Z., He, W., Yang, G., Lv, Z., Yu, Y., Zheng, Y., 2016. Micheliolide inhibits LPS-induced inflammatory response and protects mice from LPS challenge. Sci. Rep. 6 (1).

Qureshi, N., Morrison, D.C., Reis, J., 2012. Proteasome protease mediated regulation of cytokine induction and inflammation. Biochim. Biophys. Acta 1823 (11), 2087–2093.

Salas, A., Hernandez-Rocha, C., Duijvestein, M., Faubion, W., McGovern, D., Vermeire, S., Vetrano, S., Vande Casteele, N., 2020. JAK-STAT pathway targeting for the treatment of inflammatory bowel disease. Nat. Rev. Gastroenterol. Hepatol. 17 (6), 323–337.

Salter, M., Hazelwood, R., Pogson, C.I., Iyer, R., Madge, D.J., 1995. The effects of a novel and selective inhibitor of tryptophan 2,3-dioxygenase on tryptophan and serotonin metabolism in the rat. Biochem. Pharmacol. 49 (10), 1435–1442.

Samavati, L., Rastogi, R., Du, W., Hüttemann, M., Fite, A., Franchi, L., 2009. STAT3 tyrosine phosphorylation is critical for interleukin 1 beta and interleukin-6 production in response to lipopolysaccharide and live bacteria. Mol. Immunol. 46 (8-9), 1867–1877.

Schiff, M., Takeuchi, T., Fleischmann, R., Gaich, C.L., DeLozier, A.M., Schlichting, D., Kuo, W.L., Won, J.E., Carmack, T., Rooney, T., Durez, P., Shaikh, S., Hidalgo, R.P., van Vollenhoven, R., Zerbini, C.A.F., 2017. Patient-reported outcomes of baricitinib in patients with rheumatoid arthritis and no or limited prior disease-modifying antirheumatic drug treatment. Arthritis Res. Ther. 19, 208.

Schintu, N., Zhang, X., Svenningsson, P., 2012. Studies of depression-related states in animal models of Parkinsonism. J. Parkinsons Dis. 2, 87–106.

Schwarcz, R., Bruno, J.P., Muchowski, P.J., Wu, H.-Q., 2012. Kynurenines in the mammalian brain: when physiology meets pathology. Nat. Rev. Neurosci. 13 (7), 465–477.

Shariq, A.S., Brietzke, E., Rosenblat, J.D., Pan, Z., Rong, C., Ragguett, R.M., Park, C., McIntyre, R.S., 2018. Therapeutic potential of JAK/STAT pathway modulation in mood disorders. Rev. Neurosci. 30, 1–7.

Takahashi, K., Nakagawasai, O., Nemoto, W., Odaira, T., Sakuma, W., Onogi, H., Nishijima, H., Furihata, R., Nemoto, Y., Iwasa, H., Tan-No, K., Tadano, T., 2019. Effect of Enterococcus faecalis 2001 on colitis and depressive-like behavior in dextran sulfate sodium-treated mice: involvement of the brain-gut axis. J. Neuroinflammation 16, 201.

Theiss, A.L., Laroui, H., Obertone, T.S., Chowdhury, I., Thompson, W.E., Merlin, D., Sitaraman, S.V., 2011. Nanoparticle-based therapeutic delivery of prohibitin to the colonic epithelial cells ameliorates acute murine colitis. Inflamm. Bowel Dis. 17 (5), 1163–1176.

Tzeng, H.-T., Chyuan, I.-T., Lai, J.-H., 2021. Targeting the JAK-STAT pathway in autoimmune diseases and cancers: A focus on molecular mechanisms and therapeutic potential. Biochem. Pharmacol. 193, 114760.

Villarán, R.F., Espinosa-Oliva, A.M., Sarmiento, M., De Pablos, R.M., Argüelles, S., Delgado-Cortés, M.J., Sobrino, V., Van Rooijen, N., Venero, J.L., Herrera, A.J., Cano, J., Machado, A., 2010. Ulcerative colitis exacerbates lipopolysaccharide-induced damage to the nigral dopaminergic system: potential risk factor in Parkinson's disease. J. Neurochem. 114, 1687–1700.

Yang, L., Huh, J.R., Choi, G.B., 2023. One messenger shared by two systems: How cytokines directly modulate neurons. Curr. Opin. Neurobiol. 80, 102708.

Yoon, S., Woo, S.U., Kang, J.H., Kim, K., Shin, H.-J., Gwak, H.-S., Park, S., Chwae, Y.-J., 2012. NF-κB and STAT3 cooperatively induce IL6 in starved cancer cells. Oncogene 31 (29), 3467–3481.

Zhao, B., Wu, J., Li, J., Bai, Y., Luo, Y., Ji, B., Xia, B., Liu, Z., Tan, X., Lv, J., Liu, X., 2020. Lycopene Alleviates DSS-Induced Colitis and Behavioral Disorders via Mediating Microbes-Gut-Brain Axis Balance. J. Agric. Food Chem. 68 (13), 3963–3975.

Zhu, Z.-G., Jin, H., Yu, P.-J., Tian, Y.-X., Zhang, J.-J., Wu, S.-G., 2013. Mollugin inhibits the inflammatory response in lipopolysaccharide-stimulated RAW264.7 macrophages by blocking the Janus kinase-signal transducers and activators of transcription signaling pathway. Biol. Pharm. Bull. 36 (3), 399–406.